British Journal of Mathematics & Computer Science
19(1): 1-22, 2016; Article no.BJMCS.20358
ISSN: 2231-0851

SCIENCEDOMAIN *international*
www.sciencedomain.org

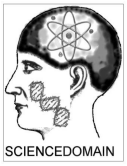

Analysis of Dynamics of HIV-1 Associated Kaposi Sarcoma during HAART and ACI

Frank Nani[1*] and Mingxian Jin[1]

[1]Department of Mathematics and Computer Science, Fayetteville State University, Fayetteville, NC 28301, USA.

Authors' contributions

This work was carried out in collaboration between both authors. Author FN constructed the clinically plausible mathematical models, based on the state-of-the-art medical literature. Author MJ performed all the computer simulations for all the patho-physiological parametric configurations. Both authors performed the mathematical analysis of the models. Both authors read and approved the final manuscript.

Article Information

DOI: 10.9734/BJMCS/2016/20358
Editor(s):
(1) Nikolaos Dimitriou Bagis, Department of Informatics and Mathematics, Aristotelian University of Thessaloniki, Greece.
Reviewers:
(1) G. Y. Sheu, Chang-Jung Christian University, Tainan, Taiwan.
(2) El Akkad Abdeslam, CRMEF Fès, Morocco.
Complete Peer review History: http://www.sciencedomain.org/review-history/16479

Original Research Article

Received: 24th July 2015
Accepted: 24th September 2016
Published: 7th October 2016

Abstract

Aims: To formulate, analyze, and perform investigative computer simulations for clinically plausible mathematical model depicting the patho-physiodynamics of HIV-1 associated Kaposi Sarcoma (KS) during Highly Active Anti-Retroviral Therapy (HAART) of AIDS and Adoptive Cellular Immunotherapy (ACI). The basic principle of digital combination therapy involving HAART and ACI is exhibited in the computer simulations.

Study Design: The mathematical model proposed in the current research is based on the results of the state-of-the-art data published in peer-reviewed journals relating to HAART, KS, and ACI. Using Dynamic Systems Theory, the clinical data is reformulated into a system of non-linear deterministic differential equations involving six model variables: non-HIV-1 infected CD4+ T lymphocytes, HIV-1 infected lymphocytes, free HIV-1 virions in the blood plasma, HIV-1 specific cytotoxic CD8+ T lymphocytes/*ex-vivo* interleukin-2 (IL-2) incubated CD8+ T cells, HAART drug molecules, and the KS cancer cells. The model incorporates all appropriate stoichiometric interaction rate coefficients, apoptotic rate constants, rate constants for viral recruitment from latent reservoirs, and other relevant parameters.

**Corresponding author: E-mail: fnani@uncfsu.edu;*

The role of CD4+ T cell-induced syncytia in modulating the outcome of HAART and ACI is exhibited in the computer simulations using clinically plausible hypothetic patient physiological parametric configurations.

Place and Duration of Study: This research was conducted at Fayetteville State University (FSU), Fayetteville, North Carolina, USA. The digital version of the model was initiated in the summer of 2015 under the HBCU Graduate STEM Summer Grant in 2015.

Methodology: The equilibrium points, also known as the physiological outcomes were computed and the local stability at these points were analyzed utilizing the Hartman-Grobman theory, the principles of linearized stability, Banach space techniques, and Lozinskii matrix based stability. The clinically desirable physiological outcomes are further analyzed to obtain plausible robust criteria under which the HIV-1 virions, HIV-1 infected CD4+ lymphocytes and KS cells are annihilated. In particular, some scenarios of therapeutic failure are also discussed.

Results: Theoretical digital criteria for remission and possible cure of KS and AIDS are derived in terms of biophysically measurable parameters. The model simulations incorporate scenarios with and without HIV-1 induced syncytia. The digital prognosis of KS and the associated HIV-1 AIDS are exhibited in terms of biophysically measurable mathematical criteria. In particular, the computer simulations use hypothetical patient parametric configurations to elucidate the quantitative dynamics of KS and associated HIV-1 AIDS during HAART and ACI.

Conclusion: This research has demonstrated that under certain patient parametric configurations, a higher density of syncytia prevents reconstitution of CD4+ T cells at various doses of HAART drug cocktail. It also establishes theoretically it is possible for HAART to annihilate HIV-1 infected CD4+ T cells and HIV-1 virions without necessarily eliminating KS.

Keywords: Kaposi Sarcoma (KS); mathematical modeling; HAART efficacy; computer simulations; ACI of KS.

1 Introduction

The Kaposi Sarcoma associated Herpes Virus 8 (KSHV-8) is a subset of the γ-herpesvirus subfamily which comprises of two subgroups namely lymphocryptovirus and rhadinovirus [1-5]. The virus is also named KSHV-8 or HHV-8 since it is the eighth known Human Herpes virus. The KSHV DNA sequences are found only in the KS tissues and not in normal tissues [4]. In particular, KSHV can be isolated in all KS lesions and localized in the vascular endothelial cells and prevascular spindle-shaped cells [4]. The gene products of KSHV-8 are homologous to cellular oncogenes and can modify the cellular cycle, inhibit apoptosis, evade immune system signaling mechanisms, and induce angiogenesis, immortalization of cancer cells, and facilitates neo-vascularization, in HIV-1 patients [3-7].

Systemic treatment of KS in AIDS patients must confront both KS and the underlying AIDS. Thus Highly Active Anti-Retroviral Therapy (HAART) chemotherapy, Adoptive Cellular Immunotherapy (ACI), and radiotherapy are the treatment modalities [6]. Since the multifocality of AIDS associated KS is the major purpose of therapy, chemotherapy and radiotherapy are often times preferred by medical and clinical oncologists. The lesions of KS are radiosensitive but adverse effects such as residual hypopigmentation, radio-dermatitis, and skin ulceration could be incapacitating to the patient. In order to minimize toxicity, intralesional cytotoxic chemotherapy is favored than whole body systemic chemotherapy. Thus innovative pegylated liposomal anthracycline anti-tumor antibiotic doxorubicin is used in first line traditional radiotherapy and immuno-therapy such as to reduce systemic toxicity. The relevance of HAART in KS therapy depends on the therapeutic efficacy of the components of the HAART protocol such as the protease inhibitors, nucleoside/non-nucleoside reverse transcriptase inhibitors and HIV-1 receptor/co-receptor inhibitors [6,7]. Localized HIV-1 associated KS may involve the use of treatment modalities such as (i) cryotherapy using liquefied nitrogen (ii) conformal radiotherapy (brachytherapy) (iii) photodynamic therapy involving photosensitizers (Photofrin II) and laser therapy.

The rationale for using ACI in HIV-1 associated KS therapy is based on clinical observation involving the use of recombinant interleukin 2 (rIL-2). The mechanism of action of rIL-2 is based on the lymph proliferative activation of CD8+ T (tumoricidal T-lymphocytes), NK (natural killer cells) and LAK (lymphokine activated killer cells) [8-10]. Related clinical research on the pathophysiology of KS during HAART can be found in [9-13].

The clinical protocol of KS specific ACI involves the following procedures [9,10,14].

Step (1) The cancer patient is primed with KS vaccine followed by lymphocyte harvest. This is therapeutically possible in principle. Such procedure is discussed by Parviz et al in [8].
Step (2) Autologous T cells are harvested from the (i) peripheral blood or alternatively using (ii) draining the lymph nodes
Step (3) The autologous T cells then undergo polyclonal in-vitro activation and proliferative expansion. Antigen-specific immune function is measured. After administration of booster vaccines.
Step (4) The *ex-vivo* rIL-2 expanded CD8+ cells are re-infused into the patient after lympho-depleting chemotherapy.
Step (5) The tumor-infiltrating KS specific CD8+ T lymphocytes can be isolated and expanded *in vitro* using rIL-2 for adaptive transfer after lympho-depleting chemotherapy.

The patho-physio-dynamics of HIV-1 induced KS has been investigated by Kemény et al. [15], Lesbordes et al. [16], Zhu et al. [17], and in publications such as [18,19,20]. The cytolytic role of $CD8^+$ T lymphocytes in regulating the growth of KS has been studied by Li et al. [21] and Stebbing et al [18]. The use of ACI with activated autologous $CD8^+$ T cells incubated with rIL-2 infusion in treatment of AIDS was described by Klimas et al. [14], Touloumi et al. [19], and Urassa et al. [20]. Additional research results have been obtained by Bihl et al. [22], and Dupont et al. [13].

Nani and Jin [23] recently developed a mathematical model depicting the dynamics of KS during HAART therapy of HIV-1 induced AIDS. The Nani-Jin model is improved in this current research to include ACI therapy of KS during HAART so to incorporate the mathematical ramifications of ACI [24,25]. In particular, stability analysis of the model has been discussed and more computer simulations are presented, as compared to the previous paper.

In this paper, we present an elaborate, deterministic mathematical model and computer simulations of the patho-physio-dynamics of KS associated with AIDS during HAART. It is one of the major attempts to construct a clinically plausible mathematical model which incorporates HAART therapy, HIV-1 induced AIDS dynamics, and KS.

2 Parameters

The model variables, parameters, cytokinetic rate constants, stoichiometric coefficients, and exogenous input rate constant will be defined as specified in this section. These numerical quantities are biophysically measurable and/or clinically quantifiable. Their exact values for each patient can be estimated. The following definitions are as specified in Nani and Jin [23,26].

x_1: the number density of non-HIV-1-infected $CD4^+$ helper T-lymphocytes per unit volume at any time t
x_2: the number density of HIV-1 infected $CD4^+$ helper T-lymphocytes per unit volume at any time t
x_3: the number density of HIV-1 virions in the blood plasma per unit volume at any time t
x_4: the number density of HIV-1 specific $CD8^+$ cytotoxic T-lymphocytes per unit volume at any time t
x_5: the concentration of the chemotherapy drug and HAART drug molecules at any time t
x_6: the number of Kaposi sarcoma cancer cells in the AIDS patient at any time t during HAART
S_1: rate of supply of un-infected $CD4^+$ T-lymphocytes
S_2: rate of supply of latently infected $CD4^+$ T-lymphocytes

S_3: rate of supply of HIV-1 virions from macrophage, monocytes, microglial cells and other lymphoid tissue different from T-lymphocytes
S_4: rate of supply of $CD8^+$ T-lymphocytes from the thymus or rate of supply of ex-vivo incubated $CD8^+$ T-lymphocytes
D: rate of HAART drug infusion by transdermal delivery
a_i, b_i: constant associated with activation of lymphocytes by cytokine interleukin-2 (IL-2) (i =1, 2, 3, 4)
α_i: constant associated with HIV-1 infection of $CD4^+$ T_4 helper cells (i =1, 2, 3)
β_1: the number of HIV-1 virions produced per day by replication and budding in $CD4^+$ T_4 helper cells
β_2: rate constant associated with replication and "budding" of HIV-1 in syncytia $CD4^+$ T_4 helper cells per day per microliter (μl) and released into the blood plasma
β_3: the number of HIV-1 virions produced per day by replication and "budding" in non-syncytia $CD4^+$ T helper cells and released into the blood plasma
η_i: constant depicting the rate of which HIV-1 virions incapacitate the $CD8^+$ T_8 cytotoxic cells (i =1, 2)
(σ_0, λ_0): Michaelis-Menten metabolic rate constants associated with HAART drug elimination
(σ_i, λ_i): Michaelis-Menten metabolic rate constants associated with HAART drug pharmacokinetics (i =2, 3)
(σ_4, λ_4): Michaelis-Menten metabolic rate constants associated with cytolytic action of $CD8^+$ against Kaposi Sarcoma cancer cells
γ_4: constant depicting the cytolytic efficacy of $CD8^+$ T cells against Kaposi sarcoma cancer cells
ξ_i: cytotoxic coefficient where $0 \le \xi_i \le 1$ (i = 2, 3)
q_i: constant depicting competition between infected and un-infected $CD4^+$ T_4 helper cells (i =1, 2)
k_i: constant depicting degradation, loss of clonogenicity or "death" (i =1, 2, 3, 4, 5, 6)
e_{i0}: constant depicting death or degradation or removal by apoptosis (programmed cell death) (i =1, 2, 3, 4)
K_i: constant associated with the killing rate of infected $CD4^+$ T cells by $CD8^+$ T cytotoxic lymphocytes (i =1, 2)
All the parameters are positive
c_i: kinetic constants depicting logistic tumor growth for Kaposi sarcoma

3 Model Equations

The following system of non-linear deterministic ordinary differential equations models the patho-physiological dynamics of HIV-1 induced AIDS virions and associated Kaposi sarcoma cancer cells, $CD4^+$ (infected and non-infected) T cells, and $CD8^+$ T cells during HAART therapy.

$$\begin{cases} \dot{x}_1 = S_1 + a_1 x_1^2 e^{-b_1 x_1} - \alpha_1 x_1 x_3 - q_1 x_1 x_2 - k_1 x_1 - e_{10} \\ \dot{x}_2 = S_2 + a_2 x_1 x_2 e^{-b_2 x_1} + \alpha_2 x_1 x_3 - q_2 x_1 x_2 - k_2 x_2 - \beta_1 x_3 - K_1 x_2 x_4 - e_{20} - \dfrac{\xi_2 \sigma_2 x_2 x_5}{\lambda_2 + x_5} \\ \dot{x}_3 = S_3 + \beta_2 x_2 x_3 + \beta_3 x_3 - \alpha_3 x_1 x_3 - \eta_1 x_3 x_4 - k_3 x_3 - e_{30} - \dfrac{\xi_3 \sigma_3 x_3 x_5}{\lambda_3 + x_5} \\ \dot{x}_4 = S_4 + a_4 x_1 x_4 e^{-b_4 x_1} - K_2 x_2 x_4 - \eta_2 x_3 x_4 - \gamma_4 \dfrac{\sigma_4 x_4 x_6}{\lambda_4 + x_4} - k_4 x_4 - e_{40} \\ \dot{x}_5 = D\left|\lceil \sin nt \rceil\right| - \dfrac{\sigma_0 x_5}{\lambda_0 + x_5} - \dfrac{\sigma_2 x_2 x_5}{\lambda_2 + x_5} - \dfrac{\sigma_3 x_3 x_5}{\lambda_3 + x_5} - k_5 x_5 \\ \dot{x}_6 = c_1 x_6 - c_2 x_6^2 - \dfrac{\sigma_4 x_4 x_6}{\lambda_4 + x_4} - k_6 x_6 \\ x_i(t_0) = x_{i0} \quad for \quad i = \{1, 2, 3, 4, 5, 6\} \end{cases} \tag{3.1}$$

4 Analysis of the Model Equations

In this section, the principles of non-linear system analysis will be used to derive some results on the qualitative behavior of the model equations. The mathematical techniques used for analyzing the model equations are discussed in [27,28,29,30,31].

4.1 Boundedness, dissipativity, and invariance of non-negativity

Consider the model equations (3.1). Let

$$\begin{cases} L_j = \sup\limits_{t\in[t_0,t_F]} [a_j x_1 x_j e^{-b_j x_1}] \quad for\ j=\{1,2,4\} \\ L_3 = \sup\limits_{t\in[t_0,t_F]} [\beta_2 x_2 x_3 + \beta_3 x_3] \end{cases} \tag{4.1}$$

where t_0 and t_F denote respectively the time for commencement and termination of HAART and ACI therapy.

The system of differential equations (3.1) reduce to the following system of differential inequalities.

$$\begin{cases} \dot{x}_1 \le S_1 + L_1 - k_1 x_1 - e_{10} \\ \dot{x}_2 \le S_2 + L_2 - k_2 x_2 - e_{20} \\ \dot{x}_3 \le S_3 + L_3 - k_3 x_3 - e_{30} \\ \dot{x}_4 \le S_4 + L_4 - k_4 x_4 - e_{40} \\ \dot{x}_5 \le D - k_5 x_5 \\ \dot{x}_6 \le d x_6 - c_2 x_6^{\,2} \quad where\ d = c_1 - k_6 \end{cases} \tag{4.2}$$

$$\begin{cases} x_1(t_0) = x_{10} \\ x_2(t_0) = x_{20} \\ x_3(t_0) = x_{30} \\ x_4(t_0) = x_{40} \\ x_5(t_0) = x_{50} \\ x_6(t_0) = x_{60} \end{cases} \tag{4.3}$$

$$x_{i0} \in \Re^5{}_+ = \{x_i \in \Re \mid x_i \ge 0\}$$

Integrating the system (4.2), the following dynamical inequalities are obtained.

$$\begin{cases} x_1(t) \le \dfrac{S_1 + L_1 - e_{10}}{k_1} + r_1 e^{-k_1 t} \\ x_2(t) \le \dfrac{S_2 + L_2 - e_{20}}{k_2} + r_2 e^{-k_2 t} \\ x_3(t) \le \dfrac{S_3 + L_3 - e_{30}}{k_3} + r_3 e^{-k_3 t} \\ x_4(t) \le \dfrac{S_4 + L_4 - e_{40}}{k_4} + r_4 e^{-k_4 t} \\ x_5(t) \le \dfrac{D}{k_5} + r_5 e^{-k_5 t} \\ x_6(t) \le d x_6(0) / [c_2 x_6(0) + d - c_2 x_6(0) e^{-dt}] \end{cases} \tag{4.4}$$

where $r_i \in \Re^+ = [0, \infty)$ are constants of integration for i ={1, 2, 3, 4, 5}.

Thus

$$\begin{cases} \limsup_{t\to\infty} |x_1(t)| \le \dfrac{S_1 + L_1 - e_{10}}{k_1} \\ \limsup_{t\to\infty} |x_2(t)| \le \dfrac{S_2 + L_2 - e_{20}}{k_2} \\ \limsup_{t\to\infty} |x_{31}(t)| \le \dfrac{S_3 + L_3 - e_{30}}{k_3} \\ \limsup_{t\to\infty} |x_4(t)| \le \dfrac{S_4 + L_4 - e_{40}}{k_4} \\ \limsup_{t\to\infty} |x_5(t)| \le \dfrac{D}{k_5} \\ \limsup_{t\to\infty} |x_6(t)| \le \dfrac{d}{c_2} \end{cases} \tag{4.5}$$

The inequalities of (4.5) show that the system (3.1) is dissipative for $\frac{S_i + L_i - e_{i0}}{k_i} \neq 0$ where i={1,2.3,4.5}. We thus have the following theorem.

Theorem 4.1 Let

$$M_i = \max[x_{i0,} \frac{S_i + L_i - e_{i0}}{k_i}] \text{ for } i=\{1,2,3,4\}$$
$$\Re_+^6 = \{(x_1,...,x_6) \in \Re^6 | x_i > 0 \ \textit{for}\ i = \{1,2,3,4,5,6\}$$

Consider the set

$$A = \{x_1,..., x_6) \in \Re_+^6 \mid 0 \le x_1 \le M_1,\ 0 \le x_2 \le M_2,\ 0 \le x_3 \le M_3,\ 0 \le x_4 \le M_4,\ 0 \le x_5 \le \frac{D}{k_5},\ 0 \le x_6 \le \frac{d}{c_2}\} \tag{4.6}$$

Then the following hold

(i) The set A is non-negatively invariant
(ii) The set A is a global attractor
(iii) All solutions of (3.1) with initial values chosen in $\Re_+^6$ will eventually enter A and are ultimately bounded and remain entrapped in A for all $t \in \Re_+$.

Proof. The proof follows directly from the preceding calculations leading to the theorem. Also see [27] Theorem 3.1 for details of the proof.

4.2 Existence of an *mT* periodic solution

It will be shown in this subsection that (3.1) admits an *mT* periodic solution, where *m* is an integer and *T* is the period.

The non-linear system (3.1) can be rewritten in the form:

$$\begin{cases} \dot{x} = A(t)x + F(t,x) \\ x(t_0) = x_0,\ x \in \Re^6 \end{cases} \tag{4.7}$$

where

$$\begin{aligned} &\text{(i)} \quad F \in C^1(\Re_+ \times \Re^6, \Re^6) \\ &\text{(ii)} \quad A \in M_6(\Re) \\ &\text{(iii)} \quad F(t+T, x) = F(t,x) \\ &\text{(iv)} \quad F(t, x) \text{ is locally Lipschitz, and} \\ &\text{(v)} \quad \|F(t,x)\| \le M \quad \text{for some } M > 0 \end{aligned} \tag{4.8}$$

In particular,

$$A(t) = \begin{bmatrix} -k_1 & 0 & 0 & 0 & 0 & 0 \\ 0 & -k_2 & -\beta_1 & 0 & 0 & 0 \\ 0 & 0 & \beta_3 - k_3 & 0 & 0 & 0 \\ 0 & 0 & 0 & -k_4 & 0 & 0 \\ 0 & 0 & 0 & 0 & -k_5 & 0 \\ 0 & 0 & 0 & 0 & 0 & -k_6 \end{bmatrix} \tag{4.9}$$

and

$$F(t,x) = \begin{bmatrix} S_1 + a_1 x_1^2 e^{-b_1 x_1} - \alpha_1 x_1 x_3 - q_1 x_1 x_2 - e_{10} \\ S_2 + a_2 x_1 x_2 e^{-b_2 x_1} + \alpha_2 x_1 x_3 - q_2 x_1 x_2 - K_1 x_2 x_4 - e_{20} - \dfrac{\xi_2 \sigma_2 x_2 x_5}{\lambda_2 + x_5} \\ S_3 + \beta_2 x_2 x_3 - \alpha_3 x_1 x_3 - \eta_1 x_3 x_4 - e_{30} - \dfrac{\xi_3 \sigma_3 x_3 x_5}{\lambda_3 + x_5} \\ S_4 + a_4 x_1 x_4 e^{-b_4 x_1} - K_2 x_2 x_4 - \eta_2 x_3 x_4 - \gamma_4 \dfrac{\sigma_4 x_4 x_6}{\lambda_4 + x_4} - e_{40} \\ D\left|\lceil \sin nt \rceil\right| - \dfrac{\sigma_0 x_5}{\lambda_0 + x_5} - \dfrac{\sigma_2 x_2 x_5}{\lambda_2 + x_5} - \dfrac{\sigma_3 x_3 x_5}{\lambda_3 + x_5} \\ c_1 x_6 - c_2 x_6^2 - \dfrac{\sigma_4 x_4 x_6}{\lambda_4 + x_4} \end{bmatrix} \tag{4.10}$$

Theorem 4.2 Consider the model equations as rewritten in (4.7). Suppose that conditions (i) – (iv) in (4.8) hold. Then there exists an *mT* periodic solution of (4.7), if $\beta_3 < k_3$.

***Proof*:**

Step 1. Consider the system

$$\dot{u} = A(t)u \quad \text{where} \quad A \in M_6(\Re) \tag{4.11}$$

The eigen-spectrum of $A(t)$ is defined by

$\sigma(A,\lambda) = \{\lambda \mid \det(A - \lambda I) = 0\} = \{-k_1, -k_2, \beta_3 - k_3, -k_4, -k_5, -k_6\}$ under the theorem hypothesis $\dot{\mu} = A(t)\mu$.

All the eigen-values of A has negative real parts. It means that all solutions of (4.11) tend to zero as t $\to \infty$.

Step 2. The next step is to show that if solution of (4.11) are uniformly ultimately bounded

Let the solution of (4.11) be denoted by $u(t, t_{0,} x_0)$. The solutions are uniformly bounded with bound M if there exist positive constants B1, B2, such that for $t_0 \in R_+$, $\| x_0 \| \leq B_1$, $t \geq t_0 + B_2$, then $\| u(t, t_0, x_0) \| < M$ [27].

Using Floquet theory, there exists a T-periodic matrix $P(t)$ and a constant matrix J such that $X(t) = P(t)e^{Jt}$ is the principal matrix solution of (4.11). But solutions of (4.11) tend to zero as $t \to \infty$.

If $u(t) = u(t,0,x_0)$ such that $f(t,u(t)) = g(t)$ is a non-homogeneous term with $|g(t)| \leq M > 0$. Using the variation of parameters formula, we have the following:

$$|x(t)| = P(t)e^{Jt}x_0 + \int_0^t P(t)e^{J(t-s)}P^{-1}(s)g(s)ds \tag{4.12}$$

Let $\left|e^{Jt}\right| \leq \alpha e^{-\beta t}$ *where* $\alpha, \beta > 0$

$$c_1 = \sup |P(t)|$$
$$c_2 = \sup \left|P^{-1}(t)\right|$$

Thus $\limsup |x(t, t_0, x_0)| \leq \dfrac{c_1 c_2 \alpha M}{\beta}$

Therefore, all solutions are uniformly ultimately bounded. Hence, there exist an mT periodic solution [27].

4.3 Linearized stability of the model equations

In this section, the stability of the model equations will be analyzed for the scenario in which the periodic input $D\left|\lceil \sin nt \rceil\right|$ is replaced by a constant drug input D.

The Jacobian matrix of linearization of (3.1) in the neighborhood of an arbitrary equilibrium point E=[x_{10}, x_{20}, x_{30}, x_{40}, x_{50}, x_{60}] has the form:

$$J(E) = \{a_{ij}\} \text{ where } 1 \le i,\ j \le 6$$

$$\dot{u} = \{J(E[x_{10}, x_{20}, x_{30}, x_{40}, x_{50}, x_{60}])\}u \text{ where } u = x - x_{k0} \text{ and } 1 \le k \le 6 \text{ and } u \in \Re^6$$

In particular,

$$\begin{aligned}
a_{11} &:= a_1 x_1 (2 - b_1 x_1) e^{-b_1 x_1} - \alpha_1 x_3 - q_1 x_2 - k_1 \\
a_{12} &:= -q_1 x_1 \\
a_{13} &:= -\alpha_1 x_1 \\
a_{14} &:= 0 \\
a_{15} &:= 0 \\
a_{16} &= 0 \\
a_{21} &:= a_2 x_2 (1 - b_2 x_1) e^{-b_2 x_1} - q_2 x_2 \\
a_{22} &:= a_2 x_1 e^{-b_2 x_1} - q_2 x_1 - k_2 - K_1 x_4 - \frac{\xi_2 \sigma_2 x_5}{\lambda_2 + x_5} \\
a_{23} &:= \alpha_2 x_1 - \beta_1 \\
a_{24} &:= -K_1 x_2 \\
a_{25} &:= -\frac{\xi_2 \lambda_2 \sigma_2 x_2}{(\lambda_2 + x_5)^2} \\
a_{26} &= 0\, a_{26} = 0 \\
a_{31} &:= -\alpha_3 x_3 \\
a_{32} &:= \beta_2 x_3 \\
a_{33} &:= \beta_2 x_2 + \beta_3 - \alpha_3 x_1 - \eta_1 x_4 - k_3 - \frac{\xi_3 \sigma_3 x_5}{\lambda_3 + x_5} \\
a_{34} &:= -\eta_1 x_3 \\
a_{35} &:= -\frac{\xi_3 \sigma_3 \lambda_3 x_3}{(\lambda_3 + x_5)^2} \\
a_{36} &= 0 \\
a_{41} &:= a_4 x_4 (1 - b_4 x_1) e^{-b_4 x_1} \\
a_{42} &:= -K_2 x_4 \\
a_{43} &:= -\eta_2 x_4 \\
a_{44} &:= a_4 x_1 e^{-b_4 x_1} - K_2 x_2 - \eta_2 x_3 - k_4 \\
a_{45} &:= 0 \\
a_{46} &= -\frac{\gamma_4 \sigma_4 x_4}{\lambda_4 + x_4} \\
a_{51} &:= 0 \\
a_{52} &:= -\frac{\sigma_2 x_5}{\lambda_2 + x_5} \\
a_{53} &:= -\frac{\sigma_3 x_5}{\lambda_3 + x_5} \\
a_{54} &:= 0 \\
a_{55} &:= -\frac{\sigma_0 \lambda_0}{(\lambda_0 + x_5)^2} - \frac{\sigma_2 \lambda_2 x_2}{(\lambda_2 + x_5)^2} - \frac{\sigma_3 \lambda_3 x_3}{(\lambda_3 + x_5)^2} - k_5 \\
a_{56} &= 0
\end{aligned} \tag{4.13}$$

$$a_{61} := 0$$
$$a_{62} := 0$$
$$a_{63} := 0$$
$$a_{64} := -\frac{\sigma_4 \lambda_4 x_6}{(\lambda_4 + x_4)^2}$$
$$a_{65} := 0$$
$$a_{66} := c_1 - 2c_2 x_6 - \frac{\sigma_4 x_4}{\lambda_4 + x_4} - k_6$$

4.4 Analysis of the equilibrium $E[\bar{x}_1, 0, 0, \bar{x}_4, \bar{x}_5, 0]$

In this subsection the clinically desirable physiologically outcome $E[\bar{x}_1, 0, 0, \bar{x}_4, \bar{x}_5, 0]$ will be analyzed using the linearized system explained in Section 4.2. This therapeutic disease equilibrium corresponds to the scenario in which the HIV-1 infected CD4+ T cells, plasma HIV-1 virions, and neoplastic KS cells are obliterated by combination of HAART and palliative chemotherapy. The necessary conditions for the local existence of this equilibrium are the following:

$$\begin{cases} S_1 + a_1 \bar{x}_1^2 e^{-b_1 \bar{x}_1} - k_1 \bar{x}_1 - e_{10} = 0 \\ S_i - e_{i0} = 0 \quad i = \{2,3\} \\ S_4 + a_4 \bar{x}_1 \bar{x}_4 e^{-b_4 \bar{x}_1} - k_4 \bar{x}_4 - e_{40} = 0 \\ D - \frac{\sigma_0 \bar{x}_5}{\lambda_0 + \bar{x}_5} - k_5 \bar{x}_5 = 0 \quad for \ \ \bar{x}_1, \bar{x}_4, \bar{x}_5 \in \Omega \end{cases} \tag{4.14}$$

$$J\{E[x_1,0,0,x_4,x_5,0]\} =$$
$$\begin{bmatrix} a_1 x_1 (2-b_1 x_1) e^{-b_1 x_1} - k_1 & -q_1 x_1 & -\alpha_1 x_1 & 0 & 0 & 0 \\ 0 & a_2 x_1 e^{-b_2 x_1} - q_2 x_1 - k_2 - K_1 x_4 - \frac{\xi_2 \sigma_2 x_5}{\lambda_2 + x_5} & \alpha_2 x_1 - \beta_1 & 0 & 0 & 0 \\ 0 & 0 & \beta_3 - \alpha_3 x_1 - \eta_1 x_4 - k_3 - \frac{\xi_3 \sigma_3 x_5}{\lambda_3 + x_5} & 0 & 0 & 0 \\ a_4 x_4 (1-b_4 x_1) e^{-b_4 x_1} & -K_2 x_4 & -\eta_2 x_4 & a_4 x_1 e^{-b_4 x_1} - k_4 & 0 & -\frac{\gamma_4 \sigma_4 x_4}{\lambda_4 + x_4} \\ 0 & -\frac{\sigma_2 x_5}{\lambda_2 + x_5} & -\frac{\sigma_3 x_5}{\lambda_3 + x_5} & 0 & -\frac{\sigma_0 \lambda_0}{(\lambda_0 + x_5)^2} - k_5 & 0 \\ 0 & 0 & 0 & 0 & 0 & c_1 - \frac{\sigma_4 x_4}{\lambda_4 + x_4} - k_6 \end{bmatrix} \tag{4.15}$$

Definition Let $T := \frac{d}{dx}$ be the Frechet differential operator such that

$$T: \Re^n \to \Re^n$$
$$F(x) \to [DF(x)]_{nxn} := A = [a_{ij}] \ where \ 1 \le i, j \le n$$

where $F(x)$ is the nonlinear vector-valued function given by the right hand side of Equation (3.1). In particular $[DF(x_0)]$ is the Jacobian matrix of linearization of (3.1) in the neighborhood of the equilibrium point $x_0 \in \Re^6$.

Note that $\Re^n$ equipped with the p-norm is a finite dimensional Banach space for $1 \le p \le \infty$.

$$T(\alpha x + \beta y) = \alpha Tx + \beta Ty$$

$$\exists k \geq 0 \text{ such that } \|T\| \leq K\|x\| \quad \text{and}$$
$$\|T\| = \sup_{\|x\| \leq 1} \|Tx\|$$

Thus $T x = A x \quad x \in \Re^n$ and T is a linear operator.

Let $1 \leq p \leq \infty$ and define the Lebesgue ℓ^p norm [28] on $\Re^n$ as

$$\|x\|_{\ell^p} = (|x_1|^p + |x_2|^p + ... + |x_n|^p)^{1/p} \quad \textit{for } 1 \leq p < \infty$$

where
$$\|x\|_{\ell^1} = |x_1| + |x_2| + ... + |x_n|$$
$$\|x\|_{\ell^2} = (|x_1|^2 + |x_2|^2 + ... + |x_n|^2)^{1/2}$$
$$\|x\|_{\ell^\infty} = \max\{|x_1|, |x_2|, ... |x_n|\}$$

It can be shown that all the above norms on $\Re^n$ are equivalent.

Let

$$\|A\| = \sup_j \sum_i |a_{ij}|$$

Then the Lozinskii matrix measure of *A* is defined as:

$$\mu(A) = \sup_j \left\{ R_e a_{jj} + \sum_{i, i \neq j} |a_{ij}| \right\}$$

Let

$$A = J\{E[x_1, 0, 0, x_4, x_5, 0]\} = \{a_{ij}\} \textit{ where } 1 \leq i, j \leq 6$$

Using the entries of *A* as defined in (4.15), $\mu(A)$ is computed as follows.

$$\begin{aligned}
&\mu(A) = \sup_j \left\{ R_e a_{jj} + \sum_{i, i \neq j} |a_{ij}| \right\} \\
&= \sup\{ a_{11} + |a_4 x_4 (1 - b_4 x_1) e^{-b_4 x_1}|, \\
&\quad a_{22} + q_1 x_1 + K_2 x_4 + \frac{\sigma_2 x_5}{\lambda_2 + x_5}, \\
&\quad a_{33} + \alpha_1 x_1 + |\alpha_2 x_1 - \beta_1| + \eta_2 x_4 + \frac{\sigma_3 x_5}{\lambda_3 + x_5}, \\
&\quad a_{44} + \frac{\sigma_4 \lambda_4 x_6}{(\lambda_4 + x_4)^2}, \\
&\quad a_{55} + \frac{\xi_3 \sigma_3 \lambda_3}{(\lambda_3 + x_5)^2}, \\
&\quad a_{66} + \frac{\gamma_4 \sigma_4 x_4}{\lambda_4 + x_4} \}
\end{aligned} \tag{4.16}$$

Assume that the parametric configuration of a hypothetical AIDS patient is such that the following specifications can be made:

$$
\begin{aligned}
&x_1 = \frac{1}{b_4} = \frac{\beta_1}{\alpha_2} \\
&K_1 = K_2 \\
&\xi_2 = \xi_3 = 1 \\
&q_1 = q_2 \\
&\eta_1 = \eta_2 \\
&\alpha_1 = \alpha_3 \\
&\gamma_4 = 1
\end{aligned}
\tag{4.17}
$$

Then Equation (4.16) reduces to

$$
\begin{aligned}
\mu(A) = \sup\{ & a_1 x_1 (2 - b_1 x_1) e^{-b_1 x_1} - k_1, \\
& a_2 x_1 e^{-b_2 x_1} - k_2, \\
& \beta_3 - k_3, \\
& a_4 x_1 e^{-b_4 x_1} - k_4, \\
& -\frac{\sigma_0 \lambda_0}{(\lambda_0 + x_5)^2} - k_5, \\
& c_1 - k_6 \}
\end{aligned}
\tag{4.18}
$$

We the have the following theorems.

Theorem 4.3.1 Suppose

$$
\begin{aligned}
&\text{(i)} \quad x_1 > \frac{2}{b_1} \\
&\text{(ii)} \quad a_2 x_1 e^{-b_2 x_1} - k_2 < 0 \\
&\text{(iii)} \quad \beta_3 - k_3 < 0 \\
&\text{(iv)} \quad a_4 x_1 e^{-b_4 x_1} - k_4 < 0 \\
&\text{(v)} \quad c_1 - k_6 < 0
\end{aligned}
\tag{4.19}
$$

Then the solution trajectory of the model equations (3.1) in the ε-neighborhood of $E[x_1, 0, 0, x_4, x_5, 0]$ is uniformly asymptotically stable.

Comments on Theorem

This theorem demonstrates the existence of a scenario in which the HIV-1 infected CD4+ T cells, HIV-1 virions, and Kaposi Sarcoma cells are annihilated using continuation of HAART and adoptive immunotherapy with ex-vivo incubated CD8+ T cells.

Proof: Consider the expression (4.16), using the specifications (4.17) and Theorem 4.1.2 in Kartsatos [28], it can be immediately concluded that $E[x_1, 0, 0, x_4, x_5, 0]$ is uniformly asymptotically stable if $\mu(A) \leq -r$ where r is a positive real number.

Theorem 4.3.2 Suppose

$$\begin{aligned}
&\text{(i)} \quad a_1 x_1 (2 - b_1 x_1) e^{-b_1 x_1} - k_1 < 0 \\
&\text{(ii)} \quad a_2 x_1 e^{-b_2 x_1} - q_2 x_1 - k_2 - K_1 x_4 - \frac{\xi_2 \sigma_2 x_5}{\lambda_2 + x_5} < 0 \\
&\text{(iii)} \quad \beta_3 - \alpha_3 x_1 - \eta_1 x_4 - k_3 - \frac{\xi_3 \sigma_3 x_5}{\lambda_3 + x_5} < 0 \\
&\text{(iv)} \quad a_4 x_1 e^{-b_4 x_1} - k_4 < 0 \\
&\text{(v)} \quad c_1 - \frac{\sigma_4 x_4}{\lambda_4 + x_4} - k_6 < 0
\end{aligned} \tag{4.20}$$

Then $E[x_1,0,0,x_4,x_5,0]$ is a local attractor.

Proof: Consider the Jacobian matrix (4.15) which is a linearization of the non-linear model equations (3.1) in the ε-neighborhood of $E[x_1,0,0,x_4,x_5,0]$. By the Hartman-Grobman theorem [29], the flow associated with the non-linear system is C^0-conjugate to that of the linearized system $\dot{u} = \{J(E[x_1,0,0,x_4,x_5,0])\}u$ where $u = x - x_0, u \in \Re^6$ in the neighborhood of $E[x_1,0,0,x_4,x_5,0]$.

An inspection of the Jacobian matrix (4.15) reveals that the eigenvalues given by the following expressions:

$$\begin{aligned}
\lambda_1 &= a_1 x_1 (2 - b_1 x_1) e^{-b_1 x_1} - k_1 \\
\lambda_2 &= a_2 x_1 e^{-b_2 x_1} - q_2 x_1 - k_2 - K_1 x_4 - \frac{\xi_2 \sigma_2 x_5}{\lambda_2 + x_5} \\
\lambda_3 &= \beta_3 - \alpha_3 x_1 - \eta_1 x_4 - k_3 - \frac{\xi_3 \sigma_3 x_5}{\lambda_3 + x_5} \\
\lambda_4 &= a_4 x_1 e^{-b_4 x_1} - k_4 \\
\lambda_5 &= -\frac{\sigma_0 \lambda_0}{(\lambda_0 + x_5)^2} - k_5 \\
\lambda_6 &= c_1 - \frac{\sigma_4 x_4}{\lambda_4 + x_4} - k_6
\end{aligned}$$

Conditions (i) ~ (v) of the theorem guarantee that all the eigenvalues have negative real parts. Using the principles of linearized stability [29], it can be concluded that $E[x_1,0,0,x_4,x_5,0]$ is a hyperbolic sink and locally asymptotically stable and a local attractor.

5 Digital Prognostic Simulations

In this section, hypothetical patient physiological parametric configurations are used to illustrate some aspects of the dynamics of Kaposi Sarcoma (KS) during HAART and ACI. The parametric values used in the simulations are estimates based on values presented in the following papers [23,26]. For all the simulations below, the units of x_i are cells/μl for i =1,2,4,5,6 and virions/μl for i = 3. The time axis unit is year.

The convergence of the simulations is guaranteed by the following theorem [31]:

Theorem 5.1 Consider the initial value problem.

$$\begin{cases} \dot{x} = f(t,x) \quad t \in [t_0, t_0 + \alpha] \quad \alpha > 0 \\ x(t_0) = x_0 \end{cases} \tag{5.1}$$

where $f \in C(\Re_+ \times \Re^n, \Re^n)$ and $x_0 \in \Re^n$

Let (5.1) be rewritten in the iterative form as follows.

$$\begin{cases} y_{k+1} = y_{i+h}\phi(t_i, y_i, h) \quad for\ h > 0, i \in N \\ y_0 = x_0 \quad y_0 \in \Re^n, x_0 \in \Re^n \end{cases}$$

If there is a value $h_0 > 0$ such that $\phi(t,y,h)$ is continuous on the domain

$$D = \{t, y, h \mid t \in [t_0, t_0 + \alpha], y \in \Re^n, h \in [0, h_0]\}$$

And if there exists a constant $L > 0$ such that

$$|\phi(t,y,h) - \phi(t,\bar{y},h)| \le L|y - \bar{y}|$$

For all $(t,y,h),(t,\bar{y},h) \in D$ called a Lipschitz condition, then the following hold:

(i) The numerical algorithm is stable

(ii) The algorithmic scheme is convergent if and only if it is consistent, that is, if and only if $\phi(t,x,0) = f(t,x,0) \quad \forall\, t \in [t_0, t_0 + \alpha]$

(iii) If the local truncation errors are bounded by $|\tau_i| \le B(h)$ for some function $B(h)$, independent of i and for $h \in [0, h_0]$, then $|x(t_i) - y_i| \le \dfrac{B(h)e^{L(t_i - t_0)}}{L}$ where L is the local Lipschitz constant.

5.1 Simulation for hypothetical KS patient #1

Suppose the hypothetical AIDS/KS patient has parametric configuration P_1 as exhibited in Table 1.

The parametric configuration for P_1' is similar to that of P_1 except that $\beta_2 = 0.01$ (with moderate syncytia) vs. $\beta_2 = 0$ (absence of syncytia). The cancer growth rate constant for both P_1 and P_1' is set to $c_1 = 6.405$. The simulation results are shown in Fig. 1.

An inspection of the output graphs show that the effect of non-zero syncytia is relevant to the dynamics of CS8+ T cells (x4), but there is no marked effect on the other dynamic variables. The effect of no-zero syncytia is to decrease the number of CD8+ T cells. It can be observed from the simulation results that the immune system of the patient is reconstituted during the HAART and ACI therapy.

5.2 Simulation for hypothetical KS patient #2

The effect of KS growth rates for fixed syncytia level and fixed HAART drug does rate D is investigated in this simulation. The parametric configuration of the hypothetical patient #2 is shown in Table 2. In parametric configuration P_2', the only changes are as follows: $c_1 = 6.405$ instead of $c_1 = 10.25$.

Table 1. Hypothetical AIDS patient parametric configuration P_1

x_{10} = 500 cells/μl	x_{20} = 400 cells/μl	x_{30} = 1000 virions/μl	x_{40} = 1500 cells/μl	x_{50} = 1500 cells/μl	x_{60} = 2500 cells/μl
S_1 = 800 /day/μl	S_2 = 800 /day/μl	S_3 = 10 /day/μl	S_4 = 2000 /day/μl	n = 5	c_1 = 6.405
e_{10} = 0.0025 cells/day/μl	e_{20} = 0.0005 cells/day/μl	e_{30} = 0.0001 /day	e_{40} = 0.0002	D = 4000 units	c_2 = 0.00075
a_1 = 0.15 /day/cell/μl	a_2 = 0.11 /day/cell/μl	β_2=0.01 virions/CD4$^+$/day/μl	cells/day/μl	σ_0 = 0.5 *mg*/day	σ_4 = 7 *mg*/day
b_1 = 0.01 /cell/μl	b_2 = 0.004/cell/μl	β_3 = 2.75 virions/CD4$^+$/day	a_4 = 0.35 /day/cell/μl	σ_2 = 30 *mg*/day	k_6=0.0025/day/μl
α_1 = 0.5/day/virions/μl	α_2= 0.5/day/virions/μl	α_3 = 0.027 /day/virions/μl	b_4 = 0.01/cell/μl	σ_3 = 5 *mg*/day	λ_4 = 5.5 *mg/L*
k_1 = 0.0005/day/μl	k_2 = 0.005/day/μl	k_3 = 0.0001/day/μl	K_2 = 0.0024 /day/μl	k_5=0.001/day/μl	
q_1 = 0.00045/day/μl/cell	q_2 = 0.00001/day/μl/cell	η_1 = 0.055	k_4 = 0.08/day/μl	λ_0 = 5 *mg/L*	
	β_1 = 1.5 virions/CD4$^+$/day	ξ_2 = 0.85	η_2 = 0.055	λ_2 = 10 *mg/L*	
	K_1 = 0.0001/day/μl	ξ_3 = 0.0001	γ_4 = 0.15	λ_3 = 0.015 *mg/L*	

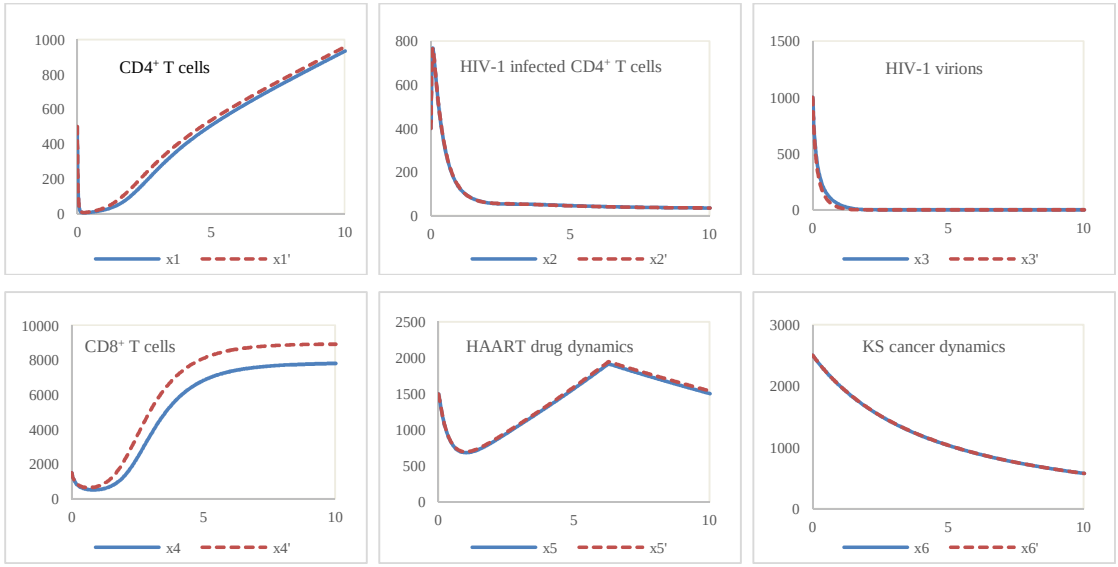

Fig. 1. Simulation results using parametric configurations P_1 vs. P_1'

(P_1' is the modified P_1: same as P_1 except $\beta_2 = 0$ instead of $\beta_2 = 0.01$. The time axis unit is year.)

Table 2. Hypothetical AIDS patient parametric configuration P_2

x_{10} = 500 cells/μl	x_{20} = 400 cells/μl	x_{30} = 1000 virions/μl	x_{40} = 1500 cells/μl	x_{50} = 1500 D = 4000 units	x_{60} = 2500 cells
S_1 = 800 /day/μl	S_2 = 800 /day/μl	S_3 = 10 /day/μl	S_4 = 2000 /day/μl	σ_0 = 0.5 *mg*/day	c_1 = 10.25
e_{10} =	e_{20} = 0.0005 cells/day/μl	e_{30} = 0.0001 /day	e_{40} = 0.0002	σ_2 = 30 *mg*/day	c_2 = 0.00075
0.0025 cells/day/μl	a_2 = 0.11 /day/cell/μl	β_2=0 virions/CD4$^+$/day/μl	cells/day/μl	σ_3 = 5 *mg*/day	σ_4 = 7 *mg*/day
a_1 = 0.15 /day/cell/μl	b_2 = 0.004/cell/μl	β_3 = 2.75 virions/CD4$^+$/day	a_4 = 0.35 /day/cell/μl	k_5=0.001/day/μl	k_6=0.0025/day/μl
b_1 = 0.01 /cell/μl	α_2= 0.5/day/virions/μl	α_3 = 0.027 /day/virions/μl	b_4 = 0.01/cell/μl	λ_0 = 5 *mg/L*	λ_4 = 5.5 *mg/L*
α_1 = 0.5/day/virions/μl	k_2 = 0.005/day/μl	k_3 = 0.0001/day/μl	K_2 = 0.0024 /day/μl	λ_2 = 10 *mg/L*	
k_1 = 0.0005/day/μl	q_2 = 0.00001/day/μl/cell	η_1 = 0.055	k_4 = 0.08/day/μl	λ_3 = 0.015 *mg/L*	
q_1 = 0.00045/day/μl/cell	β_1 = 1.5 virions/CD4$^+$/day	ξ_2 = 0.85	η_2 = 0.055	cells/μl	
	K_1 = 0.0001/day/μl	ξ_3 = 0.0001	γ_4 = 0.15	n = 5	

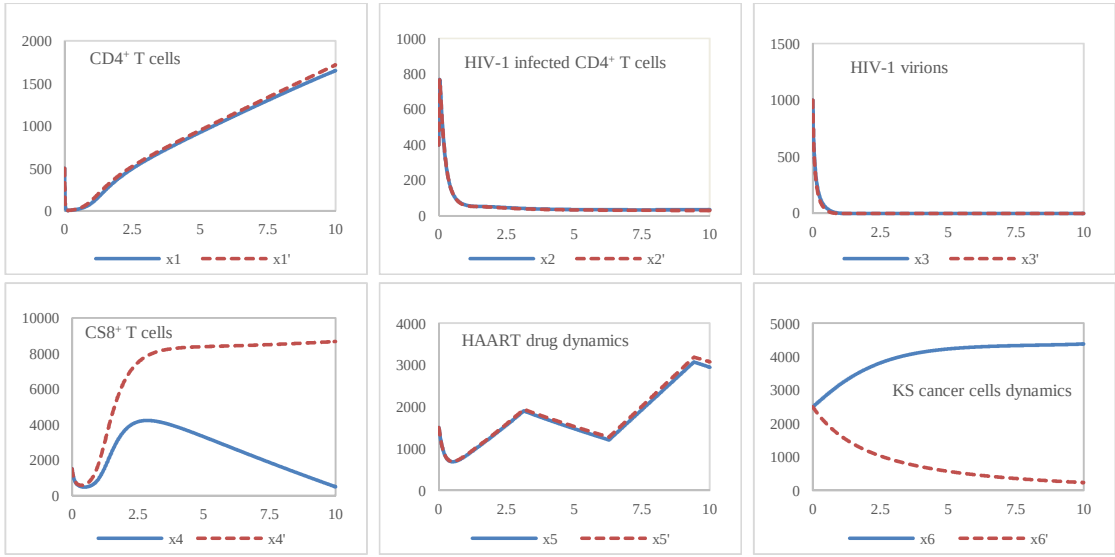

Fig. 2. Simulation results using parametric configurations P_2 vs. P_2'

(P_2' is the modified P_2: same as P_2 except c_1 = 6.405 instead of c_1 = 10.25. The time axis unit is year.)

Table 3. Hypothetical AIDS patient parametric configuration P_3

S_1 = 800 /day/μl	S_2 = 800 /day/μl	S_3 = 10 /day/μl	S_4 = 2000 /day/μl	D = 4000 units	c_1 = 10.25
a_1 = 0.15 /day/cell/μl	a_2 = 0.11 /day/cell/μl	β_2=0.01 virions/CD4$^+$/day/μl	a_4 = 0.35 /day/cell/μl	σ_0 = 0.5 *mg*/day	c_2 = 0.00075
b_1 = 0.01 /cell/μl	b_2 = 0.004/cell/μl	β_3 = 2.75 virions/CD4$^+$/day	b_4 = 0.01/cell/μl	σ_2 = 30 *mg*/day	σ_4 = 7 *mg*/day
α_1 = 0.5/day/virions/μl	α_2= 0.5/day/virions/μl	α_3 = 0.027 /day/virions/μl	K_2 = 0.0024 /day/μl	σ_3 = 5 *mg*/day	k_6=0.0025/day/μl
k_1 = 0.0005/day/μl	k_2 = 0.005/day/μl	k_3 = 0.0001/day/μl	k_4 = 0.08/day/μl	k_5=0.001/day/μl	λ_4 = 5.5 *mg/L*
q_1 = 0.00045/day/μl/cell	q_2 = 0.00001/day/μl/cell	e_{30} = 0.0001 /day	e_{40} = 0.0002	λ_0 = 5 *mg/L*	x_{60} = 2500cells
e_{10} = 0.0025 cells/day/μl	β_1 = 1.5 virions/CD4$^+$/day	η_1 = 0.055	cells/day/μl	λ_2 = 10 *mg/L*	
x_{10} = 500 cells/μl	K_1 = 0.0001/day/μl	ξ_2 = 0.85	η_2 = 0.055	λ_3 = 0.015 *mg/L*	
	e_{20} = 0.0005 cells/day/μl	ξ_3 = 0.0001	γ_4 = 0.15	x_{50} = 1500 cells/μl	
	x_{20} = 400 cells/μl	x_{30} = 1000 virions/μl	x_{40} = 1500 cells/μl	n = 5	

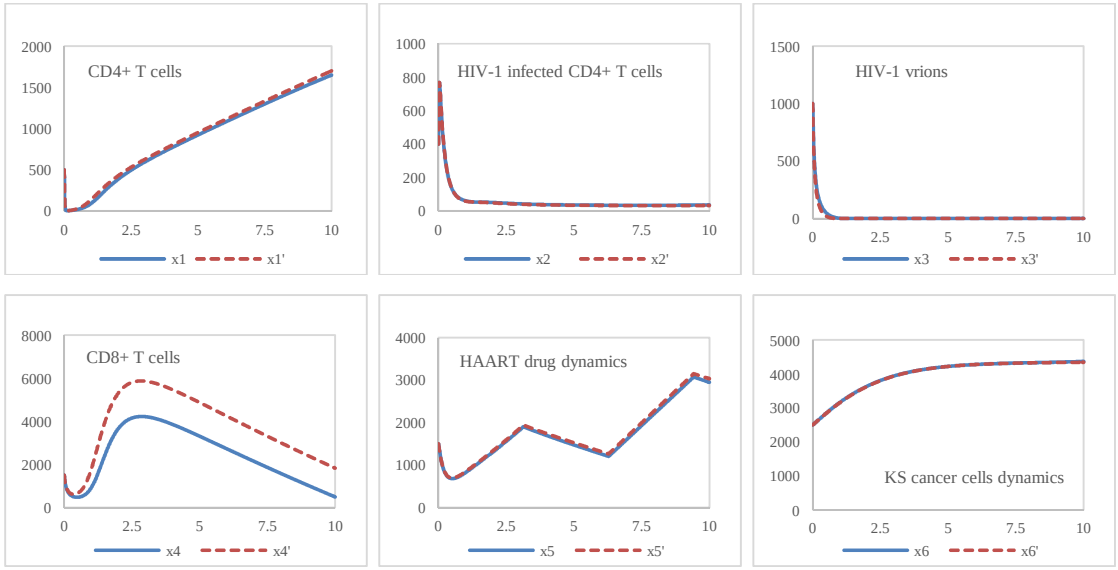

Fig. 3. Simulation results using parametric configurations P_3 vs. P_3'

(P_3' is the modified P_3: same as P_3 except $\beta_2 = 0$ instead of $\beta_2 = 0.01$. The time axis unit is year.)

Table 4. Hypothetical AIDS patient parametric configuration P_4

S_1 = 800 /day/μl	S_2 = 800 /day/μl	S_3 = 10 /day/μl	S_4 = 2000 /day/μl	D = 4000 units	c_1 = 10.25
a_1 = 0.15 /day/cell/μl	a_2 = 0.11 /day/cell/μl	β_2=0.03 virions/CD4$^+$/day/μl	a_4 = 0.35 /day/cell/μl	σ_0 = 0.5 *mg*/day	c_2 = 0.00075
b_1 = 0.01 /cell/μl	b_2 = 0.004/cell/μl	β_3 = 2.75 virions/CD4$^+$/day	b_4 = 0.01/cell/μl	σ_2 = 30 *mg*/day	σ_4 = 7 *mg*/day
α_1 = 0.5/day/virions/μl	α_2= 0.5/day/virions/μl	α_3 = 0.027 /day/virions/μl	K_2 = 0.0024 /day/μl	σ_3 = 5 *mg*/day	k_6=0.0025/day/μl
k_1 = 0.0005/day/μl	k_2 = 0.005/day/μl	k_3 = 0.0001/day/μl	k_4 = 0.08/day/μl	k_5=0.001/day/μl	λ_4 = 5.5 *mg/L*
q_1 = 0.00045/day/μl/cell	q_2 = 0.00001/day/μl/cell	e_{30} = 0.0001 /day	e_{40} = 0.0002	λ_0 = 5 *mg/L*	x_{60} = 2500cells
e_{10} = 0.0025 cells/day/μl	β_1 = 1.5 virions/CD4$^+$/day	η_1 = 0.055	cells/day/μl	λ_2 = 10 *mg/L*	
x_{10} = 500 cells/μl	K_1 = 0.0001/day/μl	ξ_2 = 0.85	η_2 = 0.055	λ_3 = 0.015 *mg/L*	
	e_{20} = 0.0005 cells/day/μl	ξ_3 = 0.0001	γ_4 = 0.15	x_{50} = 1500 cells/μl	
	x_{20} = 400 cells/μl	x_{30} = 1000 virions/μl	x_{40} = 1500 cells/μl	n = 5	

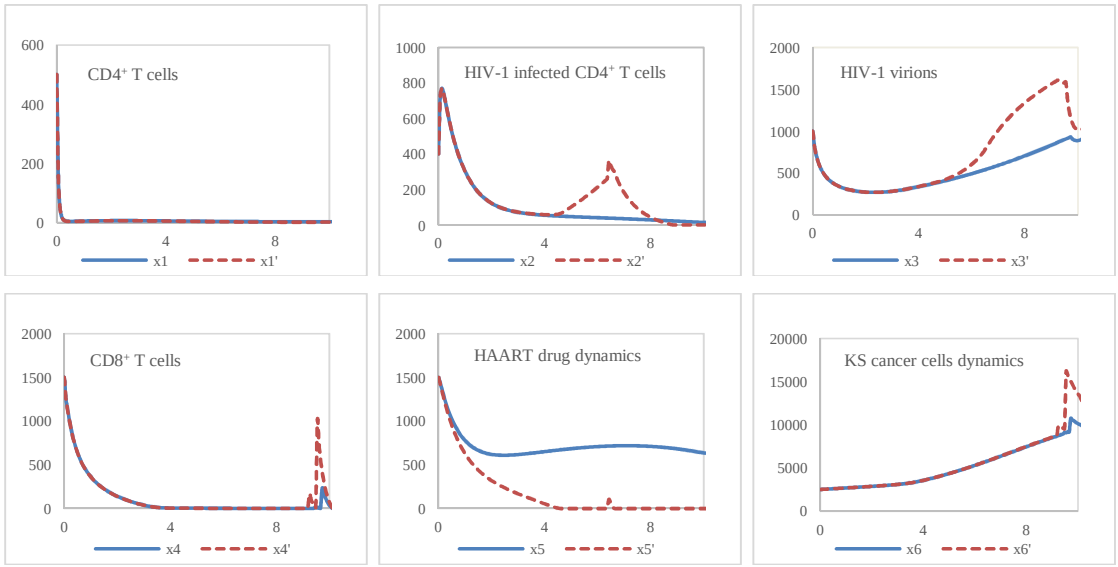

Fig. 4. Simulation results using parametric configurations P_4 vs. P_4'

(P_4' is the modified P_4: same as P_4 except D = 1000 instead of D = 4000. The time axis unit is year.)

It can be observed from Fig. 2 that the adoptively transferred ex-vivo IL2 incubated CD8+ T cells with the dose rate D of 4000 units of HAART drug and the ACI ex-vivo CD8+ T cells (S_4 = 2000) were comparatively effective in reducing the growth rate of KS cells which have the lower value of c_1 = 6.405 as compared to the KS cells with the higher value of c_1 = 10.25. It can also be observed from the simulation results that the immune system of the patient is reconstituted during the HAART and ACI therapy.

5.3 Simulation for hypothetical KS patient #3

The effect of non-zero syncytia is investigated in this section. A hypothetical patient #3 with parametric configuration P_3 with non-zero syncytial rate (β_2 = 0.01) is compared to a hypothetical patient P_3' with zero syncytial rate (β_2 = 0). For both patients, c_1 = 10.25, and D = 4000 are fixed.

The simulation results show that the difference between the digital prognoses of the hypothetical patients are negligible except for the dynamics of CD8+ (x_4) T cells In particular, the peak of the CD8+ for zero syncytia is lower than that of non-zero syncytia. Also it is possible to compare the results with those of Section 5.1. In section 5.1, the dynamics of the CD8+ cells have an asymptotic configuration after t = 5 as compared to the dynamics of CD8+ cells in section 5.2 that show a rapidly decreasing rate after t = 5. In addition, the dynamics of KS is concave up and concave down respectively in sections 5.1 and 5.2. It can be observed from the simulation results that the immune system of the patient is reconstituted during the HAART and ACI therapy.

5.4 Simulation for hypothetical KS patient #4

The effect of HAART drug dose rate is investigated in this section. The hypothetical patient #4 is subject to two dose regimes of HAART drug with respective dose rates of D = 4000 (P_4) and D = 1000 (P_4'). The syncytial rates are kept fixed at β_2=0.03 and the KS growth rate is fixed at c_1 = 10.25.

The simulation results in Figure 4 show the following:

(i) The digital prognosis for the two scenarios is poor because the non-infected CD4+ T cells are annihilated in both cases.
(ii) The dynamics of the CD HIV-1 infected CD4+ T cells is such that the rate for t = 4 to t = 8 shows a spike for the lower dose rate of D = 1000.
(iii) The HIV-1 virions dynamics exhibits a marked spike for D =1000 emanating at t =6 that peaks at t = 10.
(iv) The effect of a higher HAART dose on KS is negligible except for a spike in KS growth rate at t =10.
(v) With a non-zero and higher syncytia rate, the immune system is not reconstituted at either D= 4000 or D =1000. In particular, the non-infected CD4+ T cells are annihilated in both dose regimes.

6 Summary and Future Work

The results presented in this paper can be summarized in the following statements:

(i) It is possible, in principle, for HAART to annihilate HIV-1 infected CD4+ T cells and HIV-1 virions without necessarily eliminating KS.
(ii) ACI with adoptively transferred tumor infiltrating CD8+ T cells can lead to remission in KS inpatients with HIV-1 induced AIDS who are undergoing HAART.
(iii) The combined use of ACI and HAAART can lead to immune reconstitution of CD4+ T cells as seen in simulations with hypothetical patient #2. This effect is confirmed by the work of Bihl et al. in [22].

(iv) Under certain patient parametric configurations, a higher density of syncytia, as indicated by a higher value of β_2, prevents reconstitution of CD4+ T cells at various doses of HAART drug cocktail. This effect was observed in hypothetical patient #4.

The major difficulty associated with this model is the determination and estimation of the physiologic interaction constants and stoichiometric coefficients. It is possible to obtain or estimate most of them by statistical analysis of biophysical data from *in-vitro* experiments or *in-vivo* animal or human data.

In future a more plausible formulation of the syncytia will be attempted in which the quadratic term $\beta_2 x_2 x_3$ will be remodeled. The model equations (3.1) will be refurbished with appropriate time delays which are associated with HIV-1 latency. Another feature of the future model will be the inclusion of time lags involved in ACI therapy. In particular, more investigative simulations will be presented.

Disclaimer

A portion of this manuscript without the mathematical analysis nor ACI therapy and with different computer simulations was presented in the conference "International Conference on Bioinformatics and Computational Biology 2011 (BIOCOMP'11)," available link is "https://www.researchgate.net/publication/259889749_Dynamics_of_HIV-1_Associated_Kaposi_Sarcoma_during_HAART_Therapy" dated on July 2011 in Las Vegas, NV.

Competing Interests

Authors have declared that no competing interests exist.

References

[1] Moore PS, Gao SJ, Dominguez G, et al. Primary characterization of a herpesvirus agent associated with Kaposi's Sarcoma. J. Virol. 1996;70(1):549-558.

[2] Chang Y, Moore PS. Kaposi's Sarcoma (KS) –associated herpes virus and its role in KS. Infecto Agents Dis. 1996;5(4):215-222.

[3] Antman K, Chang Y. Kaposi Sarcoma. N. Engl. J. Med. 2000;342:1027-1038.

[4] Szajerka T, Jablecki J. Kaposi Sarcoma revisited. AIDS Review. 2007;9:230-236.

[5] Cattelan AM, Calabro ML, De Rossi. Long term clinical outcome of AIDS related Kaposi Sarcoma during HAART. International Journal of Oncology. 2005;27(3):779-785.

[6] Sato E, Olson SH, et al. Intraepithelial CD8+ tumor infiltrating lymphocytes and a high CD8+/regulatory T cell radio are associated with favorable prognosis of ovarian cancer. Pro. Natl. Acad. Sci. USA. 2005;102(51):18538-18543.

[7] Wrzesinski C, Paulos CM, Rosenberg SA, et al. Hematopoietic stem cells promote the expansion and function of adoptively transferred anti-tumor CD8+ T cells. J. Clin. Invest. 2007;117(2):492-501.

[8] Parviz M, Chin CS, Graham LJ, et al. Successful adotive immunotherapy with vaccine-sensitized T cells, despite the effect of no vaccination alone in a weakly immunogenic tumor model. Cancer Immunology Immunotherapy. 2003;52(12):739-750.

[9] Dupin N, Rubin de Cervens V, Gorin I, et al. The influence of highly active anti-retroviral therapy on AIDS-associated Kaposi Sarcoma. Br. J. Dermatol. 1999;140:875-881.

[10] Lebbe C, Blum L, Pellet C, et al. Clinical and biological impact of anti-retroviral therapy with protease inhibitors on HIV-related Kaposi Sarcoma. AIDS. 1998;12:F45-F49.

[11] Tavio M, Nasti G, Spina M, Errante D, et al. Highly active anti-retroviral therapy in HIV-related Kaposi Sarcoma. Ann. Oncol. 1998;9:923.

[12] Martinez V, Caumes E, Gambotti L, et al. Remission from Kaposi Sarcoma on HAART is associated with suppression of HIV replication and s independent of protease inhibitor therapy. British Journal of Cancer. 2006;94:1000-1006.

[13] Dupont C, Vasseur E, Beauchet A, Aegerter P, et al. Long term efficacy on Kaposi Sarcoma of highly active anti-retroviral therapy in a cohort of HIV-positive patients. AIDS. 2000;14:987-993.

[14] Klimas N, et al. Clinical and immunological changes in AIDS patients following adoptive therapy with activated autologous CD8 T cells and interlukin-2 infusion. AIDS. 1994;8(8):1073-81.

[15] Kemény L, et al. Human herpes virus 8 in classic Kaposi sarcoma. Acta Microbiologica et immunologica Hungarica. 1996;43(4):391-395.

[16] Lesbordes JL, et al. Clinical and histopathological aspects of Kaposi's sarcoma in Africa: relationship with HIV serology. Annales de I'Institut Pasteur, Virology. 1988;139(2):197-203.

[17] Zhu B, Wu NP, Hoxtermann S, Bader A, Brockmeyer N. Immune activation in AIDS related Kaposi's sarcoma. Zhejiang da xue xue bao = Journal of Zhejiang University, Medical Science. 2003;32(2): 101-103.

[18] Stebbing J, Sanitt A, Teague A, Powles T, Nelson M, Gazzard B, Bower M. CD8 count measurement has independent prognostic significance in individuals with AIDS-Kaposi sarcoma. Journal of Clinical Oncology, 2007 ASCO Annual Meeting Proceedings Part I. 2007;2518S(Supplement):20500.

[19] Touloumi G, et al. The role of immunosuppression and immune-activation in classic Kaposi's sarcoma. International Journal of Cancer. 1999;82(6):817-21.

[20] Urassa WK, et al. Immunological profile of endemic and epidemic Kaposi's sarcoma patients in Dar-es-Salaam, Tanzania. International Journal of Molecular Medicine. 1998;1(6):979-82.

[21] Li T, Qiu Z, Wang A, Sheng R. T-lymphocyte immune in HIV-infected people and AIDS patients in China. Zhonghua Yi Xue Za Zhi. 2002;82(20):1391-5.

[22] Bihl F, et al. Kaposi's sarcoma-associated herpes virus-specific immune reconstitution and antiviral effect of combined HAART/chemotherapy in HIV clade C-infected individuals with Kaposi's sarcoma. AIDS (London, England). 2007;21(10):1245-1252.

[23] Nani F, Jin M. Dynamics of HIV-1 associated Kaposi Sarcoma during HAART therapy. Int'l Conf. Bioinformatics and Computational Biology (BIOCOMP'11). 2011;II:783-786.

[24] Nani F, Oguztoreli MN. Modeling and simulation of Rosenberg-type adoptive cellular immunotherapy. IMA Journal of Mathematics Applied in Medicine & Biology. University of Alberta Press; 1993.

[25] Nani F, Freeman HI. A mathematical model of cancer treatment by Immunotherapy. Mathematical Biosciences. Elsevier Science Inc; 2000.

[26] Nani F, Jin M. Generalized theoretical criteria for annihilation of HIV-1 Virions during HAART. British Journal of Mathematics & Computer Science. 2015;5(2):262-299. Article no. BJMCS. 2015.018.

[27] Burton TA. Stability & periodic solutions of ordinary & functional differential equations. Dover Publications, June 3; 2005.

[28] Kartsatos AG. Advanced ordinary differential equations. Mariner Publishing Company, Inc. Tampa, Florida. 1980;60-80.

[29] Amann H. Ordinary differential equations: A introduction to nonlinear analysis. Walter De Gruypter, NY; 1990.

[30] Wiggins S. Introduction to applied nonlinear dynamical systems and chaos. Springer-Verlag, New York; 1990.

[31] David D. Eberly. Stability analysis for systems of differential equations; 2003.
Available: http://www.geometrictools.com/Documentation/StabilityAnalysis.pdf

Peer-review history:
The peer review history for this paper can be accessed here (Please copy paste the total link in your browser address bar)
http://sciencedomain.org/review-history/16479